Remote Sensing of Environment 182 (2016) 90–98

Contents lists available at ScienceDirect

Remote Sensing of Environment

journal homepage: www.elsevier.com/locate/rse

Leaf flush drives dry season green-up of the Central Amazon

Aline Pontes Lopes [a,*], Bruce Walker Nelson [a], Jin Wu [b], Paulo Maurício Lima de Alencastro Graça [a], Julia Valentim Tavares [a], Neill Prohaska [b], Giordane Augusto Martins [a], Scott R. Saleska [b]

[a] Environmental Dynamics Department, Brazil's National Institute for Amazon Research – INPA, Av. André Araújo, 2936, Manaus, AM 69067-375, Brazil
[b] Department of Ecology & Evolutionary Biology, University of Arizona, Tucson, AZ 85721, USA

ARTICLE INFO

Article history:
Received 12 August 2015
Received in revised form 30 April 2016
Accepted 15 May 2016
Available online 24 May 2016

Keywords:
Tropical forest
Dry season green-up
Enhanced Vegetation Index
Phenocam
Green Chromatic Coordinate
Leaf flush
Leaf abscission

ABSTRACT

Understanding how land surface seasonality emerges from individual tree crown phenology is a key challenge of tropical ecology. We used daily images over a full year from a tower-mounted RGB camera to quantify the leaf phenology of 267 individual tree crowns in an evergreen Central Amazon forest. The Green Chromatic Coordinate, an index of each crown's greenness, showed rapid large-amplitude positive and negative changes, each generally occurring once per year. Rapid increase was attributed to leaf flushing and occurred in 85% of all crowns. Rapid negative change occurred in 42% of individuals, caused mostly by massive pre-flush leaf abscission (31% of all crowns). Flushing was concentrated in the five driest months (55% of crowns) compared to the five wettest months (10%). Inter-crown variance of greenness was lowest in the wet season when fewer crowns were abruptly abscising or flushing leaves. With a one month lead, flushing frequency closely tracked seasonal light availability ($R = 0.89$) and was inversely correlated with rainfall ($R = -0.88$). We linked the post-flush age of each crown's leaf cohort to the Enhanced Vegetation Index (EVI) of crowns at different phenostages on a nadir view QuickBird image. When aggregated to landscape-scale, this camera-based EVI closely followed ($R = 0.95$) the MODIS MAIAC EVI of the same site, fully corrected for sun-sensor geometry effects. Leaf phenology therefore drives the dry season green-up detected by MODIS in the Central Amazon. It is also consistent with evolutionary strategies to couple photosynthetic efficiency with light availability and to avoid predation and disease on vulnerable young leaves.

1. Introduction

The response of Amazon forest phenology to seasonal precipitation, as detected by the Moderate Resolution Imaging Spectroradiometer (MODIS), has been a subject of debate (Galvão et al., 2011; Huete et al., 2006; Maeda, Heiskanen, Aragão, & Rinne, 2014; Morton et al., 2014; Saleska, Didan, Huete, & da Rocha, 2007; Saleska et al., 2016; Samanta, Ganguly, and Myneni, 2011; Xiao et al., 2005; Xiao, Hagen, Zhang, Keller, & Moore, 2006). Enhanced Vegetation Index (EVI) derived from some MODIS products, such as MOD09A1 and the MOD13 group, is not corrected for the effects of view and solar angles. View angle effects have no seasonal trend in time series and were effectively removed in an early report of dry season green-up (Huete et al., 2006) by averaging over very large sample areas. Solar zenith angle, however, does have a trend during the Central Amazon's drier months of June to September. This trend is not removed in the standard Nadir BRDF Adjusted Reflectance (NBAR) products (MCD43A4, MCD43B4), for which solar zenith angle is adjusted to local noon. From the June solstice to the September equinox, the solar zenith angle at local noon (and at the fixed times of MODIS platform passages) decreases in the Central Amazon, leading to a progressive reduction in sub-pixel shadow fraction and consequent increase in NIR reflectance and EVI (Galvão et al., 2011; Morton et al., 2014). Consequently, an apparent dry season green-up is expected in uncorrected and in NBAR-corrected products, even in the absence of true phenological causes, such as increase in total leaf area or flushing new leaves free of epiphylls (Toomey, Roberts, & Nelson, 2009; Wu et al., 2016).

Bi et al. (2015); Guan et al. (2015) and Maeda et al. (2014) have recently shown that, after fully correcting for both view and solar angle, a dry season increase in EVI is still detectable in the Central Amazon. This true dry season green-up between June and October is about one half that of uncorrected EVI, though still well above the noise level of the data (Guan et al., 2015; Saleska et al., 2016).

Independent evidence for seasonal change in Central Amazon canopy greenness is clearly relevant to this debate. An attractive alternative

* Corresponding author.
E-mail addresses: alineplopes@gmail.com (A.P. Lopes), bnelsonbr@gmail.com (B.W. Nelson), jinwu@email.arizona.edu (J. Wu), pmalencastro@gmail.com (P.M.L.A. Graça), tavares.juliav@gmail.com (J.V. Tavares), neillp@email.arizona.edu (N. Prohaska), giordanemartins@gmail.com (G.A. Martins), saleska@email.arizona.edu (S.R. Saleska).

http://dx.doi.org/10.1016/j.rse.2016.05.009
0034-4257/

is to monitor the upper canopy with tower-mounted cameras, or phenocams. These provide very high temporal frequency, useful for controlling lighting artifacts. By combining seasonal monitoring of crown-level leaf phenology stages from tower-mounted RGB phenocams with the EVI values of these same phenostages recognized in the true-color RGB space of high resolution orbital sensors that also have an NIR band, it is possible to derive the seasonal pattern of Central Amazon EVI at the landscape scale.

The study of temperate forest phenology using phenocams is well advanced (Hufkens et al., 2012; Richardson, Braswell, Hollinger, Jenkins, & Ollinger, 2009; Richardson et al., 2007; Sonnentag et al., 2012), though still improving (Yang, Tang, & Mustard, 2014). The landscape-scale annual phenological signal of a tropical evergreen forest is much more subtle than that of a deciduous temperate forest, so that lighting artifacts constitute a larger fraction of detected change. Furthermore, leaves of different ages for the same species exhibit different colors in the visible spectrum (Toomey et al., 2009; Yang et al., 2014) so that greenness indicators derived from RGB cameras are not directly correlated with leaf amount.

Here we describe the leaf phenology of a primary forest at a Central Amazon site using a full year of daily images from an RGB camera mounted ~50 m above the upper canopy. We ask the following questions:

(1) What are the seasonal patterns of leaf renewal in the upper canopy at the crown and landscape scales?
(2) Is Central Amazon leaf phenology consistent with seasonal change in the EVI detected with the MODIS satellite?

To answer our first question we develop and apply digital methods that detect very rapid changes in leaf age and amount within a crown, while minimizing artifacts related to more gradual leaf color change of mature healthy leaves, seasonal variation in light quality and instrument errors. Visual and digital detections are compared to evaluate accuracy. We also compare the monthly frequencies of rapid leaf phenology changes with monthly precipitation, photosynthetically active radiation (PAR) and soil moisture. Our second question is addressed by relating the post-flush ages of leaf cohorts in the tree crowns seen from the tower to the EVI of crown phenostages obtained from a nadir-view QuickBird image. We close with a discussion of evolutionary drivers of leaf phenology in the Central Amazon.

2. Methods

2.1. Study area and camera details

We studied an upland forest on a well-drained clay-soil plateau 150 km northeast of Manaus, Brazil, at the Amazon Tall Tower site (59.0005°W and 2.1433°S). About 600 trees and >140 tree species are found in a typical hectare (Andreae et al., 2015). The most abundant families are Lecythidaceae, Sapotaceae, Leguminosae, Burseraceae, Euphorbiaceae and Lauraceae.

We monitored the upper canopy leaf phenology from 01 July 2013 to 30 June 2014, with an RGB Stardot Netcam model XL 3MP (2048 × 1536 pixels) mounted 81 m above the ground and ~50 m above the forest canopy. The camera was controlled by a Compulab model Fit-PC2i microcomputer with heat-resistant solid-state drive. All components were installed inside weather- and insect-resistant boxes with thermal shielding and passive ventilation. The camera box was fitted with an acrylic window cleaned every four months. The camera view was west (270°), always monitoring the same crowns and excluding the sky (Fig. 1a). A 96° wide-angle lens and the high vantage point provided coverage of four hectares. Automatic exposure was turned on and automatic color balance turned off. The camera and the computer automatically rebooted and reestablished communication and settings after power losses.

2.2. Greenness metric and detection of phenostages

Greenness as used here is the Green Chromatic Coordinate of a pixel, or g_{cc} (Richardson et al., 2007; Woebbecke, Meyer, Von Bargen, & Mortensen, 1995), defined as the fractional contribution of the green channel's digital brightness value to the summed brightness values of all three RGB channels. While the g_{cc} of pixels in a leafless crown is lower than the g_{cc} of a fully leafy crown, "greenness" as measured by g_{cc} is not a direct measure of leaf amount of a crown, because g_{cc} also changes with leaf color. Gradual change in leaf color with age presents a challenge for measurement of seasonal change in landscape-scale leaf amount of a tropical forest using only RGB spectral bands.

Nonetheless, a large abrupt increase in the g_{cc} timeline of a single crown can only indicate rapid production of a new light-green leaf cohort in that crown. A large and abrupt decrease in g_{cc} within a single crown can be safely attributed to either rapid leaf loss toward a

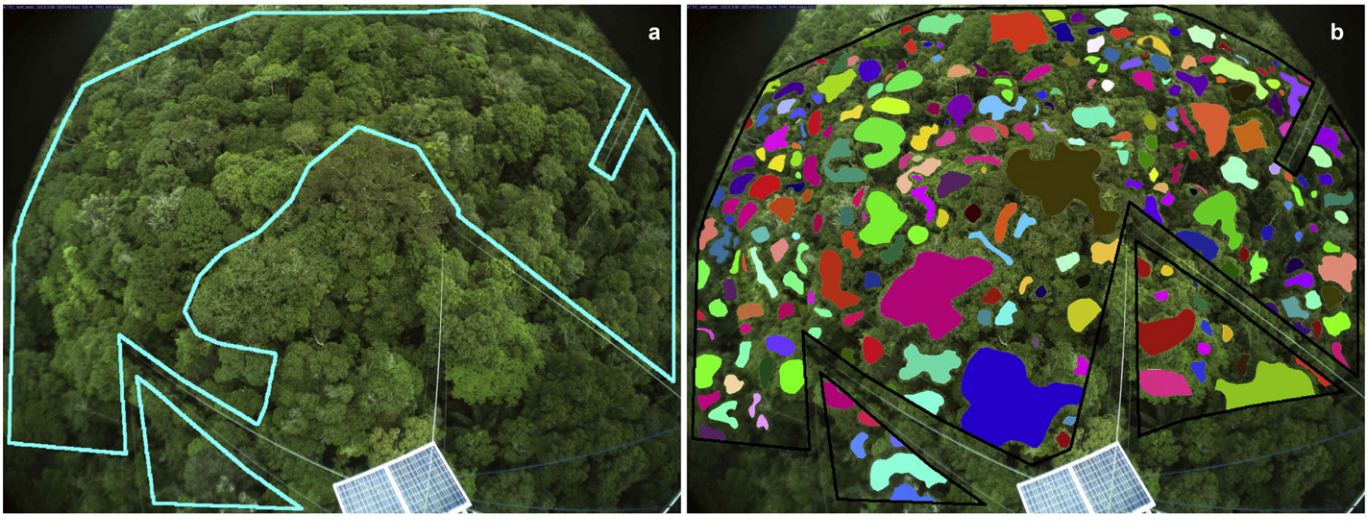

Fig. 1. Regions of interest used in digital analysis. The image area covers approximately four hectares. Radiometric intercalibration to a single reference date used the large forest area outlined in (a); corrected daily values of Green Chromatic Coordinate were then obtained for each of 267 individual crowns shown in (b).

deciduous/semi-deciduous crown state or to the earliest stage of rapid leaf flush when the crown is dominated by reddish young unexpanded leaves lacking chlorophyll. (Crowns covered with flowers, rapid massive chlorosis of old leaves and persistent dead leaves are also consistent with abrupt drop in g_{cc}, but these are infrequent on Central Amazon tree crowns.) The Excess Green Coordinate, an alternative index (Sonnentag et al., 2012), does not detect rapid green-down and proved to be noisy as it is not normalized to total pixel brightness (see Fig. S4 in Supplementary data).

Using RGB data alone, we can therefore determine seasonal abundances of three phenophases: (1) deciduous crowns plus crowns with unexpanded new leaves; (2) crowns with a recent flush of fully expanded bright green leaves free of epiphylls; and (3) crowns with dark green mature leaves or old leaves with higher epiphyll load. These stages have different post-flush ages and have distinct NIR reflectance and EVI, related to their leaf density, leaf age and epiphyll load (Toomey et al., 2009).

2.3. Removal of lighting and sensor artifacts from tower camera images

We minimized artifacts related to changing color balance of incident light, changes in shadow area and position, forward-scattered versus back-scattered illumination, diverging channel responses with different exposure speeds, sensor drift and changes of scale within the oblique view of the tower camera image. We did this by adopting a westward view and accepting photos only from 1030 to 1230 h, thus maintaining the sun behind the camera year round; by accepting only images under overcast sky (to eliminate differences in crown shadow position or size); by radiometric intercalibration of all images; and by giving equal weight to each tree crown. We selected one image per day that met our criteria. In the dry season, images with densely overcast sky are not available every day and direct light leaks through the thinner clouds. This causes variation in the incident light color balance that has a seasonal bias. Densely overcast sky in the rainy season causes longer shutter speeds and a consequent bias toward the blue channel, lowering the g_{cc}. These two image-wide seasonal biases were removed by radiometric intercalibration of all selected images against a single standard image that was obtained under an overcast sky. We adjusted the mean and the variance of each channel of each daily image to match the corresponding channel of the reference image. For this intercalibration, we selected a region of interest that excluded large tree crowns close to the camera, because phenological changes in any one of these crowns would shift the correction (Fig. 1a). Images were also geometrically adjusted so that each crown's position was stable in the daily time series.

Pre-calibration landscape-scale seasonal change in g_{cc} is of very low amplitude (Fig. 2a). This signal may be partly a consequence of seasonal change in incident color balance and in detector response at lower light levels, so was removed by the radiometric intercalibration (Fig. 2c). But this also removed any true seasonal change in average greenness across the larger forest canopy area. For this reason, and because g_{cc} changes gradually with leaf age even when leaf amount is constant (Yang et al., 2014), we do not attempt to directly measure gradual change in leaf amount at the landscape scale. We instead make a monthly census of the number of trees experiencing abrupt increase in greenness (leaf flush) and abrupt green-down (leaf abscission or very early leaf flush). These events are easily detected separately for each crown (Fig. 2b, d). From daily g_{cc} images, we extracted the average g_{cc} for each crown's

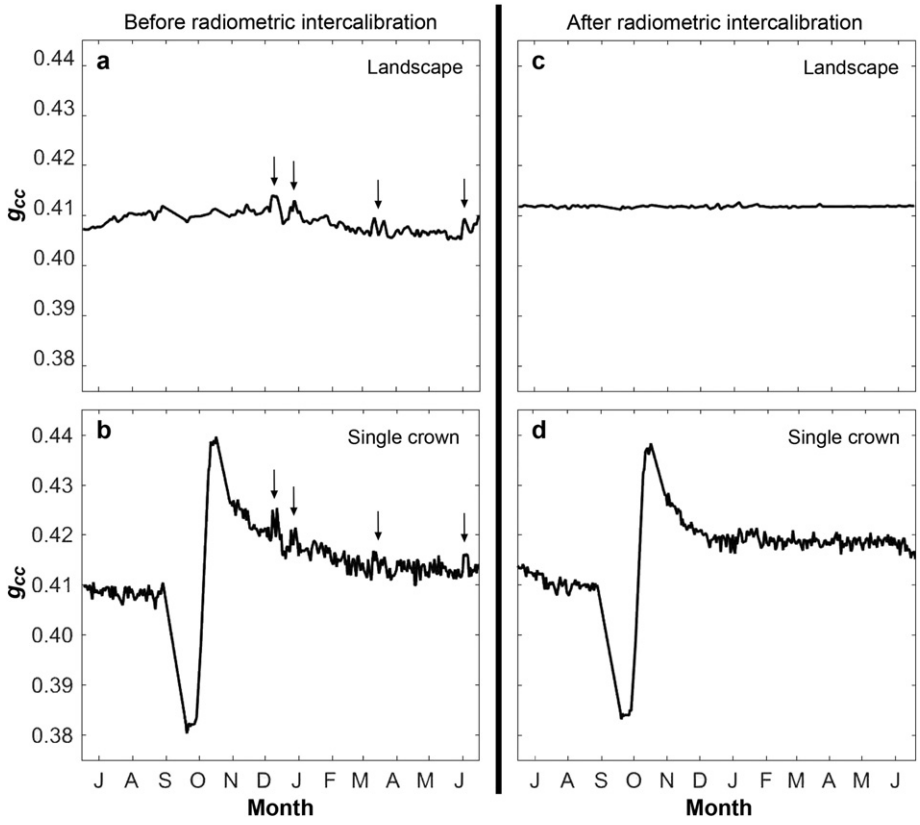

Fig. 2. Daily values of Green Chromatic Coordinate before radiometric intercalibration (panels a & b) and after (panels c & d), all with same scale. Small seasonal change in greenness of the overall forest landscape is evident in (a), but this includes any seasonal trend in incident color balance and gradual leaf color change with age, so it was removed by the radiometric intercalibration (c). Arrows in panels a and b point to the same brief artifacts caused by differences in illumination; these and the long-term gradual change of greenness in panel a, are smaller than the signals of rapid green-down and rapid leaf flush seen in the timeline of a single tree crown (large dip and large peak in panels b & d).

area and prepared an X-Y plot of the daily g_{cc} values of each crown, where Y = g_{cc}, X = day of year (as in Fig. 2d), and defined these two events as:

"Abrupt leaf flush = TRUE", if "[segment slope > 0.01 g_{cc} per month, sustained for at least 0.3 month] AND [peak of segment > percentile 0.75 of all daily observations over one year]".

"Abrupt green-down = TRUE", if "[segment slope < −0.01 g_{cc} per month, sustained for at least 0.3 month] AND [minimum of segment < percentile 0.25 of all daily observations over one year]".

Thresholds for segment slope and duration were chosen to provide results similar to a visual count of flushing crowns by month. Examples of presence or absence of flush and green-down are shown for the timelines of four crowns in Fig. S5.

2.4. Leaf flush seasonality

Abrupt leaf flush and abrupt green-down events of each crown's g_{cc} timeline were identified by the slope, duration and percentile criteria and then pegged to the date when g_{cc} of that crown reached its peak or its minimum, respectively. The number of trees at their maximum g_{cc} (leaf flush) and the number at their minimum g_{cc} were counted by month. We adjusted monthly counts to correct for data gaps, including 0.3 month gaps at the start and at the end of each crown's 12 month timeline, imposed by the slope duration criterion. System malfunctions caused three gaps in our time series of daily photos that exceeded three days in length: 13 September to 02 October, 18–22 October and 1–11 November.

To answer our first question (regarding seasonal leaf renewal patterns at the landscape scale), we compared the number of trees flushing in the five consecutive driest and the five consecutive wettest months of the year and did the same for the trees showing rapid green-down. We used chi-square to determine if these two phenomena were significantly seasonal. The fractions of all 267 trees that exhibited abrupt flushing and abrupt green-down for each month of the year were also obtained.

We also compared counts of monthly flush and of rapid green-down to monthly precipitation, photosynthetically active radiation (PAR) and soil humidity. PAR was recorded by a quantum sensor (PAR LITE, Kipp & Zonen) mounted at 75 m height on the tower. Reliable PAR data at ATTO was not available during our camera monitoring period. We instead used monthly averages of PAR for 2014–2015. PAR units are μmol photons·m^{-2}·s^{-1}. PAR flux was logged in 1 min intervals in the field. From this we obtained the average flux for each 24 h period, which was then averaged for each month of the year. Soil water was measured during the 12 months of our study at five depths between 10 and 60 cm at 10 min increments, using time-domain reflectometers (CS 615 Volumetric Water Content TDR, Campbell Scientific). We used the data from 60 cm, but all other depths showed the same seasonal pattern. Monthly precipitation was from the TRMM satellite and was averaged over the years 2003–2012, the same period as the MODIS MAIAC EVI data. We also report monthly rainfall for the 12 months of phenocam study, from a tipping bucket rain gauge (TB4, Hydrological Services) at the top of the tower.

We also determined the minimum sample size required to detect seasonal flush patterns in the Central Amazon. For each sample size from 5 to 250, we made 10,000 random draws from the full set of crowns. We ran a chi-square on each draw, comparing the number of flushing trees in the five consecutive wettest and five consecutive driest months. The sample considered sufficiently large for detecting flush seasonality (at $p = 0.05$) was that size where at least 97.5% of the random draws had at least 97.5% chi-square significance ($0.975 * 0.975 = 0.95 = 1 - p$). Non-flushing trees were included in the subsamples to give a correct result, but the chi-square test was run only on the set of trees in each run that flushed once per year.

Though we examined phenology on a crown by crown basis to understand the overall tree community, we did not examine phenology on a species by species basis. In a forest of such high diversity, only a few species – representing a small fraction of the tree community – would have sufficient replicates for meaningful interpretation of species level behavior. For example, at the Ducke Forest Reserve near Manaus, for six separate plateau forest samples of the same size as the ATTO sample, only eight tree species on average had five or more replicates. This data is available at <https://ppbio.inpa.gov.br/repositorio/dados>.

2.5. Orbital images and analysis

To answer our second question (to determine if the MODIS-detected annual behavior of EVI is consistent with our observed annual patterns of leaf phenology), we first obtained ten years of daily MODIS-MAIAC EVI for a 3 × 3 km footprint centered at the ATTO tower. The daily images were composited to biweekly intervals using an improved cloud filter, aerosol retrieval and atmospheric correction (Lyasputin et al., 2012). The biweekly mosaics were fully BRDF corrected to a standard view and solar angle. We used a ten-year average because seasonal MODIS data from Amazonia is noisy, particularly so for small footprints.

We compared the seasonal EVI pattern from MODIS to landscape-scale EVI derived from observations at the individual crown scale. For this, we obtained crown-level EVIs from a 12 August 2004 QuickBird satellite image of upland plateau forest near Manaus for three phenostages, which were known from the camera data to have different post-flush ages. These were identified on the true-color satellite image without consulting the NIR band, thus restricted to the same spectral information as in the canopy photos from the tower mounted RGB camera. We generated surface reflectance images of the four bands using the MODTRAN4 atmospheric correction as implemented in the ENVI v4.7 FLAASH module, parameterized with a tropical atmosphere model, rural aerosol model, no aerosol retrieval and 40 km initial visibility. We then applied the formula of Huete et al. (2002) to obtain the average EVI for the three phenostages of interest – ten recently flushed crowns, twenty dark green leafy crowns and twenty deciduous crowns. The deciduous class included ten crowns with light grey bare branches and ten with dark grey bare branches. We assumed crowns with unexpanded young reddish leaves had EVI similar to deciduous crowns. Because EVI is strongly affected by shadow (Galvão et al., 2011), on the QuickBird image we selected only large crowns not shaded by their neighbors. We avoided topographic shade by limiting crown selections to plateau forest, identified with the Shuttle Radar Topography Mission (SRTM) Digital Elevation Model.

The QuickBird image solar and view angles are 54° solar azimuth, 30° solar zenith, 103–140° view azimuth and 1.7° view off-nadir. It was chosen for its near-nadir view angle and lack of clouds or haze. Crowns at the three phenostages of interest were easily identified in its RGB space. The forest area used on this image is similar to that of the ATTO tower. Both are in well protected reserves of upland primary forest on well-drained clay soil plateaus, having similar rainfall amount and seasonality, and no significant disturbances that would affect EVI, such as large recent windthrows or logging.

Fig. S3 shows the tie points between QuickBird phenostage EVIs and the post-flush age of a single tree crown over a full year. The average EVI of all trees in each month gave the landscape-scale camera-based EVI seasonality. We followed a set of rules and assumptions (Text S1) for applying the QuickBird-derived EVIs to each of the 267 tree crowns at ATTO for each of the 12 months. We assumed that about half of the variance of QuickBird EVI within a sample of crowns at the same leafy phenostage is due to fine-scale age differences within that stage. Accordingly, we used the 25th, 50th and 75th percentiles of the observed QuickBird EVI from each of the two leafy phenostages to obtain a total of six predicted EVI values along the post-flush timeline of a crown. Though reasonable and justified, these simplifying assumptions and rules for constructing Fig. S3 reduce variance by an unknown amount. Reliable confidence intervals for the relationship between EVI and post-flush cohort age will require monitoring of crown reflectance

with tower-mounted hyper- or multi-spectral cameras having blue, red and NIR bands.

3. Results

The full annual amplitude of the Green Chromatic Coordinate (g_{cc}) for the forest landscape as a whole was only 0.008 units (Fig. 2a). At the individual crown scale and after radiometric intercalibration, the average g_{cc} amplitude for all 267 trees was about four times larger, 0.030 ± 0.012 units (average ± 1 sd). After radiometric intercalibration, all seasonality of g_{cc} at the landscape scale – whether real or caused by seasonal change in incoming color balance – was removed (Fig. 2c), but phenological seasonality of the landscape was then recovered by making monthly tallies of crowns experiencing rapid flush and rapid green-down.

Monthly flush counts using our digital thresholds for slope, slope duration and the position of the peaks in the crowns' g_{cc} timelines were highly correlated with monthly flush counts from visual analysis (R = 0.98 for the full set of 267 crowns; see Fig. S6). Taking the visual analysis as ground truth, the digital flush count gave a 12% omission error and an overall accuracy of 83% (Table S2).

By the digital detection method, 85% of the 267 upper canopy crowns experienced abrupt leaf flush (Table S1). Flush peaks were concentrated in the five driest months (55% of all crowns) compared to the five wettest months (10% of all crowns) a highly significant difference (chi-square$_{df1}$ = 81, p < 0.001) (Fig. 3a, Table S3a). Rapid green-down was seen in 42% of crowns. Visual checking showed that 31% of the latter were cases of rapid leaf abscission, fully or partially exposing bare branches. In order of importance, the remaining 11% were (1) a dense cohort of new reddish unexpanded leaves, (2) rapid chlorosis or death of persistent old leaves and (3) massive flowering. Rapid green-down was also more concentrated in the five driest months (26% of all crowns) versus the five wettest months (7%) (chi-square$_{df1}$ = 28, p < 0.001, Table S3b).

In the 12 August 2004 QuickBird image, average EVI vegetation indices of the three crown phenostages, which are assumed to have different post-flush ages, were all significantly different from one another (p < 0.002, Kruskal-Wallis test) (Fig. 4). Applying these QuickBird derived EVIs to the 267 trees monitored from the tower, using each crown's post-flush age at each month of the year, and then aggregating the 267 EVI values per month, provided a landscape-scale camera-based EVI with a seasonal trend (Fig. 3b). This was consistent with the dry season green-up of the Central Amazon reported by Huete et al. (2006) and Xiao et al. (2005, 2006), confirming that the latter is not an artifact of illumination geometry and is driven by leaf phenology, as also postulated by these authors. MODIS-MAIAC EVI at the ATTO tower, corrected to a standard view and illumination geometry, was also highly correlated with the camera-based EVI (R = 0.95). Camera-based EVI excluded inter-crown shadows so was consistently higher than the MAIAC EVI over an annual cycle (Fig. 3b).

Flush peak preceded the PAR peak by two months, but the two curves tracked one another very closely over the rest of the year. After imposing a one month lag on the entire flush curve, flush was strongly correlated with PAR (R = 0.89) and with monthly rainfall (R = −0.88).

Inter-crown variance of the Green Chromatic Coordinate across all 267 crowns was strongly seasonal (Fig. 5). Variance was highest in the early dry months of July and August when tree crowns were distributed more evenly among the three different phenostages that have divergent green coordinates. Crowns at the stages of pre-flush abscission (bare branches) or with reddish unexpanded leaves of early flush had low g_{cc} and all reached their peak abundance at this time of year (Fig. 3a). Mature crowns with old dark green leaves had intermediate g_{cc} and were still an abundant class at this time of year because dry season leaf flushing was just beginning. Bright green abruptly flushing crowns had high g_{cc} and also reached their peak monthly abundance

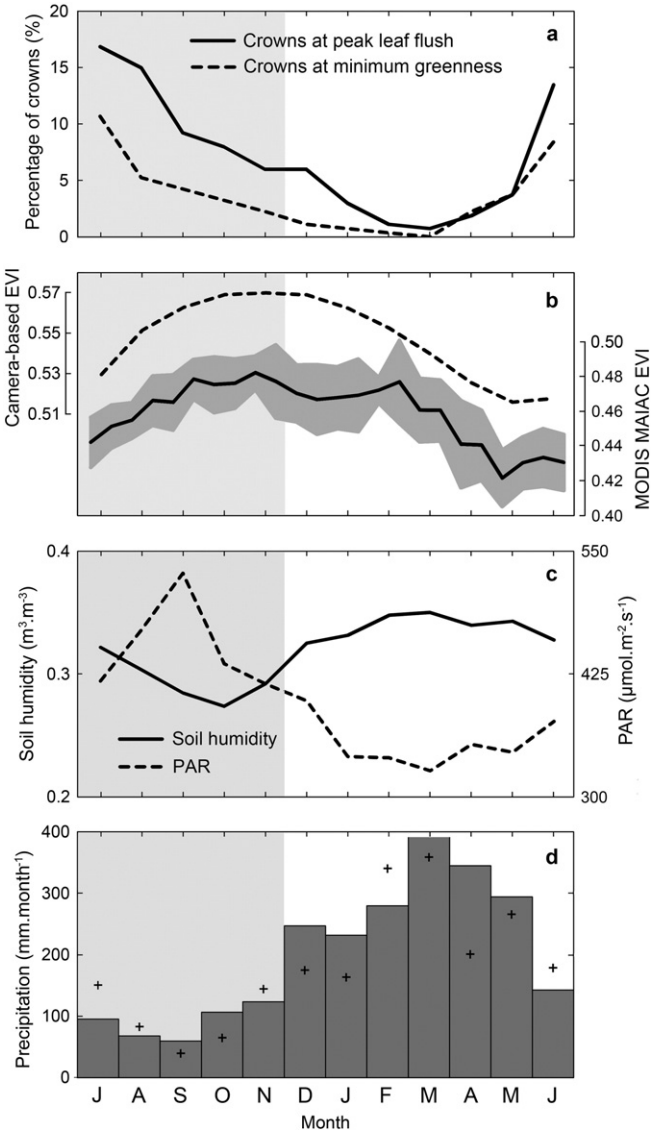

Fig. 3. Percentage of all 267 crowns with abrupt leaf flush or abrupt decrease in greenness, by month, from July 2013 to June 2014 at the Amazon Tall Tower, where grey indicates five driest months (a); monthly average of all 267 crowns' Enhanced Vegetation Index values (based on the changing mix of phenostages identified with RGB camera and the crown-scale EVI of similar phenostages in a QuickBird satellite image) compared to the ten year average of biweekly composited MODIS-MAIAC EVI for a 3 × 3 km window centered on the tower (b); monthly soil humidity from July 2013 to June 2014 and monthly averages for two years of PAR flux (c); mean monthly precipitation for ten years of TRMM data (columns) and from a rain gauge for the 12 months of phenocam data (crosses) (d).

at this time (Fig. 3a). Inter-crown variance was low in the five wettest months of January to May because leaf phenology was static, so that most crowns were of similar color, with predominantly dark green mature leaves.

A sample size of at least 40 upper canopy trees is required to detect the difference in flushing frequency between the five driest (July–November) and the five wettest months (January–May) at p = 0.05. For an overall confidence of p = 0.01, the minimum sample size is 50 trees. Therefore visual counting of monthly flushes using a much smaller sample size than the one used in this study (i.e. 267 crowns) will detect a difference between the two seasons. This can be accomplished with smaller image footprints from shorter towers.

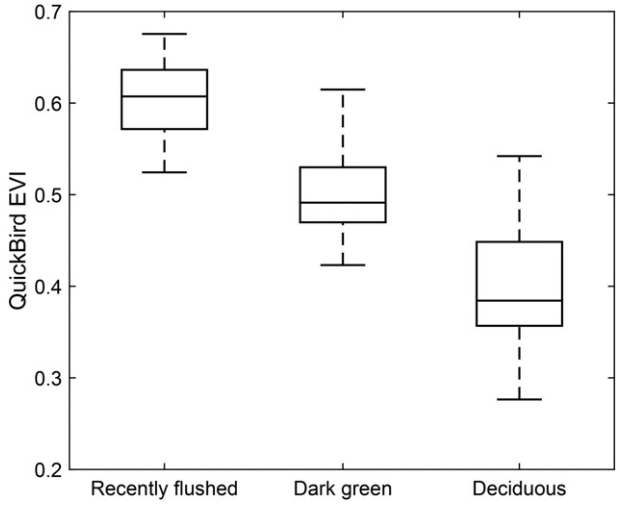

Fig. 4. Enhanced Vegetation Index of crown phenostages identified in a QuickBird true-color composite.

4. Discussion

4.1. Central Amazon leaf phenology

Similar patterns of dry season leaf flush were found for three other Central Amazon sites with upland forest on clay soil (Alencar, 1991; Brando et al., 2010; Huete et al., 2011; Nelson et al., 2014; Tavares, 2013). All studies were located 2°–3°S with dry season (monthly evapotranspiration > monthly rainfall) lasting 2–5 months. Consistently across these sites, leaf flushing occurs as a single annual peak during the drier half of the year. Each study is described below.

Alencar, Almeida and Fernandes (1979) and Alencar (1991) described leaf phenology patterns for 27 species (81 trees) monitored from the ground every month for 12 years in a Central Amazon primary upland forest (2.93°S, 59.97°W). They found that 70% (19 of 27 species) had their highest production of new leaves in the dry months, 30% (8 of 27 species) were semi-deciduous and 10% (3 of 27) were fully deciduous. Leaf flush and leaf drop were highest in the dry season, as in our study.

On a plateau at the Tapajós National Forest (2.897°S, 54.952°W), Brando et al. (2010) monitored from the ground two crown categories – having or not having new leaves – for 480 trees (>10 cm diameter at breast height) at 15 day intervals during five years. They found that ~60% of all trees had new leaves at any one time during an annual flush peak in the dry season. The precise timing of the tree community flush peak varied, but always occurred within the six driest months of July to December. In the wet season the percentage of trees with new leaves consistently dropped to ~20%. The peak and the dip were both monomodal per year. Huete et al. (2011) monitored NIR and EVI directly at this same site, using a tower-mounted ADC Tetracam, and found that both increased over the course of the five month dry season.

At the third site (2.609°S, 60.209°W, 90 km north of Manaus), ~65 crowns were monitored during 24 months using the same camera model as in our study. Expanding on the work of Tavares (2013), Nelson et al. (2014) reported that 60% of trees flushed each year, with a 4:1 ratio for flushing in the driest:wettest periods of five months. About 25% of all upper canopy crowns were fully deciduous, with abscission occurring mainly in the five driest months. As at the Amazon Tall Tower site, massive leaf drop was a preamble to leaf flush. The leafless stage was brief, lasting 36 ± 25 days. Analyses were based on visual detection of flushing events, of leaf drop events and duration of the leafless stage, using images obtained under overcast sky at six day intervals. Nelson et al. (2014) also estimated the monthly canopy leaf demography, tracking the post-flush age of each crown's leaf cohort. Though trees flush in the dry season, this causes the leaf age class with highest photosynthetic efficiency to be most abundant in the early wet season (Fig. S7).

As shown here using QuickBird EVI for different phenostages, the seasonal change in the mix of upper canopy crown stages at these three Central Amazon sites is consistent with the seasonal pattern of Enhanced Vegetation Index from the MODIS orbital sensor (e.g. Bi et al., 2015, Guan et al., 2015, Huete et al., 2006). Thus we here provide an important counterpoint to recent critiques of the detectability of seasonal increase in canopy greenness in Amazon forest canopy from June to October (Galvão et al., 2011; Morton et al., 2014). At the Amazon Tall Tower site, three crown stages with low EVI dominate the upper forest canopy in July. These are bare branches of abruptly abscising crowns, unexpanded newly flushed leaves and dark green crowns having leaves over six months of age. Visual monitoring of crowns revealed that, over the course of the previous wet season, when leaf renewal was low, these "old" crowns suffer gradual leaf attrition causing intra-crown shadows and/or partial exposure of branches. Crowns with higher epiphyll load on their leaves, with higher shadow fraction and more exposed branches will have reduced EVI (Galvão et al., 2011; Toomey et al., 2009). By the end of the five driest months, in November, most of the crowns that were at these low-EVI stages in July will have flushed and have a dense complement of fully expanded leaves with low epiphyll load. These crowns have high NIR reflectance and high EVI. This is shown both by our analysis of crown phenostages tied to those seen in the QuickBird image and by Toomey et al. (2009), using a radiative transfer model scaling up from leaf-level reflectance of Amazon tree species.

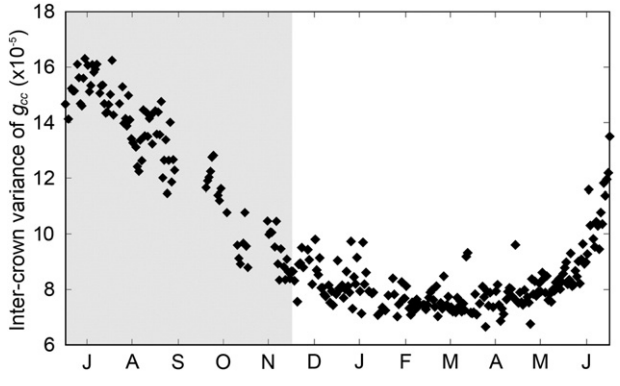

Fig. 5. Inter-crown variance of the Green Chromatic Coordinate changes with time of year. Grey indicates five driest months.

4.2. Advantages and limitations of tower mounted phenocams in tropical forests

The phenocam data collection and analysis methods described here are faster and more efficient than prior ground-based labor-intensive approaches (Richardson, Klosterman, & Toomey, 2013). Compared with airborne drones, monitoring from a tower allows the very high image frequency required to filter for diffuse illumination, which is infrequent in the dry season. A diffusely lit canopy has spatially and temporally even illumination, with no change in shadow positions or size, so less noise in a time series (Sonnentag et al., 2012). Diffusely lit images also have fewer saturated pixels, so can be radiometrically intercalibrated to further reduce noise and seasonal artifacts.

Daily, diffusely lit images allowed detection of abrupt changes in greenness in the timeline of each crown. Abrupt green-up at the crown scale has an average amplitude four times that of the image-wide seasonal green-up (Fig. 2). Therefore aggregating these strong

crown-scale patterns across hundreds of crowns provides a more robust landscape-scale measure of seasonal greenness.

Crown-scale data from towers also permit extracting seasonality of inter-crown variance in greenness, which is explained by the changing mix of phenostages. High inter-crown variance in the dry season and low variance in the wet season should be detectable in high-resolution satellite images (if obtained under nadir view and identical solar zenith angles), allowing verification and upscaling of the patterns described in this paper.

Limitations of tower mounted RGB cameras include: (1) A tower with electrical power and lightning protection is required. (2) Abrupt changes at the crown scale may go undetected where data gaps exceed about 10 days. (3) EVI cannot be measured directly. (4) Only the upper canopy is visible, so the very high percentage of flushing trees reported here may not be representative of lower canopy crowns. Leaf turnover is slower in this low light environment (Reich, Uhl, Walters, Prugh, & Ellsworth, 2004).

4.3. Drivers of Central Amazon leaf phenology patterns

What are the underlying evolutionary drivers of seasonal leaf phenology in the Central Amazon? Three hypotheses are considered below.

(1) Water stress. Flushing appears not to be limited by water availability, since it is concentrated in the months of low rainfall. Furthermore, those trees that experienced abrupt leaf drop followed by abrupt leaf flush did not delay flushing until the end of the dry season (Fig. S8). Moderate water stress cannot be precluded, however, because exchanging old leaves for new ones during the dry season may lead to improved stomatal control of water loss (Reich & Borchert, 1988). Indeed, the presence of annual rings in all Amazon upland forest trees examined (Zuidema, Brienen, & Schongart, 2012) indicates a season less favorable for wood growth, consistent with moderate water stress. Restrepo-Coupe et al. (2013), however, pointed out that wood growth remains low during the entire dry season in the Central Amazon despite photosynthesis increasing in the mid to late dry season. Slower dry season wood growth even as photosynthesis increases suggests that leaf phenology, and not water stress, drives seasonality of wood increment. Massive flush of young leaves diverts energy from wood tissue to leaf tissue formation (Restrepo-Coupe et al., 2013).

(2) Diffuse x direct incident PAR. Because newly flushed leaves require 1–2 months of maturation to reach maximum photosynthetic capacity (Kositsup et al., 2010; Yang et al., 2014), the observed lag between the July flush peak and the September PAR peak is consistent with a strategy to exploit the season of high insolation (Wright & Schaik, 1994; Xiao et al., 2006). At the community level, however, monthly changes in leaf age mix maximize landscape-scale photosynthetic capacity in the early wet season, when total incident PAR is low (Fig. 3C; also see Restrepo-Coupe et al., 2013; Wu et al., 2016) and diffuse fraction increases. Positive correlation between Gross Ecosystem Productivity and cloudiness at two eddy flux towers in the Amazon has been interpreted as showing that diffuse PAR is used more efficiently than direct PAR by the forest canopy as a whole (Cirino, Souza, Adams, & Artaxo, 2014; Oliveira et al., 2007). Leaf age structure at the community level therefore appears to be calibrated to maximize photosynthetic efficiency when light quality is at its best. However, many trees flush in the early months of the dry season. Their leaf cohorts attain maximum photosynthetic efficiency (Wu et al., 2016) when direct light fraction of PAR is still high. They remain in this physiologically efficient age bracket when the diffuse fraction of PAR is high in the early rainy season. These trees therefore appear to be indifferent to light quality.

(3) Escape from herbivores and pathogens. Leaf flush and pre-flush leaf drop concentrated in the dry season may be strategies to avoid herbivores and microbial pathogens. Young leaves are more palatable to herbivores, which are more abundant in the rainy season (Coley & Barone, 1996; Murali & Sukumar, 1993; Wright & Schaik, 1994). Young unhardened leaves are more vulnerable to fungal pathogens which are in turn favored by stable high humidity under cloudy sky and frequent rain. Two commercially important native Amazon tree species and the pathogenic microorganisms with which they have evolved provide an apt illustration. Only young unexpanded leaves of the rubber tree *Hevea brasiliensis* are susceptible to infection by the South American leaf blight fungus *Microcyclus ulei*. Infection is strongly impeded under drier climate at the southern fringe of Amazonia (Lieberei, 2007). Basidiospores of witches' broom (*Moniliophthora perniciosa*) only germinate on wet surfaces of the cocoa plant, *Theobroma cacao*. Though mature leaves can be infected, directional hyphal growth toward stomata is seen only on unhardened leaf flushes (Frias, Purdy, & Schmidt, 1991). Trees which self-prune old infected leaves prior to flushing new leaves (31% of trees in our study) may reduce nearby sources of inoculation by microbial and invertebrate pathogens. Disease control by pruning of infected tissues is common practice in tropical and temperate orchards (Azevedo et al., 2013; Marini & Burden, 1987). Detecting these evolutionary pressures in native Amazon forest may be difficult. For the two commercial species described above, natural pathogen pressures were detected when amplified by the high host densities of plantations.

5. Summary and conclusions

- Daily monitoring of the Green Chromatic Coordinate in 267 upper canopy crowns over a full year, using an RGB camera mounted on a Central Amazon tower, showed a strong seasonal pattern of leaf renewal consistent across the tree community. Rapid leaf flush and rapid pre-flush leaf drop were both concentrated in the five driest months of the year;
- With a one-month lead, both PAR and rainfall correlate strongly with flush frequency ($R = 0.89$ and -0.88, respectively);
- Enhanced Vegetation Index (EVI) at the crown scale is highest after a leaf flush and drops as the crown's leaf cohort ages. By tying phenostage EVIs from a QuickBird image to the post-flush age of each crown's leaf cohort, monitored by the tower-mounted RGB camera, it was possible to construct the annual pattern of landscape-scale EVI, which is driven by the dry season flush peak;
- Free of bias from changing view or solar illumination geometry and corrected for seasonal change in color balance, the camera- and QuickBird derived EVI serves as an independent verification of MODIS EVI;
- The seasonal pattern of camera-derived EVI was highly correlated with satellite derived MODIS-MAIAC EVI, which is fully corrected for seasonal changes in view and illumination angles. Both corroborate earlier reports of dry season green-up of the Central Amazon;
- Two tower-based and two ground-based studies at other Central Amazon upland forest sites also show dry season leaf flush, suggesting that dry season green-up is a general pattern.

Acknowledgements

We thank the Max Planck Society; the German Federal Ministry of Education and Research (BMBF contract 01LB1001A); the Brazilian Ministry of Science, Technology and Innovation (MCTI/FINEP contract 01.11.01248.00); the Amazonas State University (UEA); Amazonas State Foundation for Research (FAPEAM); the Large-scale Biosphere-Atmosphere Experiment of Brazil's National Institute for Amazon Research (LBA/INPA); and the Uatumã Sustainable Development Reserve of Amazonas State's Secretariat of Sustainable Development (SDS/CEUC/RDS-Uatumã). FAPEAM financed the GoAmazon project "Understanding the Response of Photosynthetic Metabolism in Tropical Forests to Seasonal Climate Variations". The Brazilian National Council for Technological and Scientific Development (CNPq) provided fellowships to

APL. The funders had no role in study design, data collection and analysis, decision to publish, or preparation of the manuscript. We thank Thomas Disper, Reiner Ditz and Hermes Braga Xavier of the ATTO logistics team; Marta Sá, Antonio Huxley and Leonardo Oliveira of the Micrometeorological group of LBA/INPA; Antônio Manzi and Marciel José Ferreira for logistic and financial support; and Carolina Castilho for analysis of PPBio tree inventories. Alexei Lyapustin and Yujie Wang developed the MODIS MAIAC EVI processing procedures and Kaiyu Guan helped extract ten years data for the ATTO site.

Map. KMZ file containing the Google map of the most important areas described in this article.

Appendix A. Supplementary data

Supplementary data associated with this article can be found in the online version, at doi: 10.1016/j.rse.2016.05.009. These data include the Google map of the most important areas described in this article.

References

Alencar, J. C. (1991). Estudos fenológicos de espécies florestais arbóreas e de palmeiras nativas da Amazônia. In A. L. Val, R. Figlioulo, & E. Feldberg (Eds.), *Bases científicas para estratégias de preservação e desenvolvimento da Amazônia: Fatos e perspectivas* (pp. 215–220). Manaus: Instituto Nacional de Pesquisas da Amazonia.

Alencar, J. C., de Almeida, R. A., & Fernandes, N. P. (1979). Fenologia de espécies florestais em floresta tropical úmida de terra firme na Amazonia Central. *Acta Amazonica*, *9*(1), 163–198.

Andreae, M. O., Acevedo, O. C., Araújo, A., Artaxo, P., Barbosa, C. G. G., Barbosa, H. M. J., ... Yáñez-Serrano, A. M. (2015). The Amazon Tall Tower Observatory (ATTO) in the remote Amazon Basin: Overview of first results from ecosystem ecology, meteorology, trace gas, and aerosol measurements. *Atmospheric Chemistry and Physics Discussions*, *15*(18), 11599–11726. http://dx.doi.org/10.5194/acpd-15-11599-2015.

Azevedo, F. A., Lanza, N. B., Sales, C. R. G., Silva, K. I., Barros, A. L., & De Negri, J. D. (2013). Pruning in citrus culture. *Citrus Research & Technology*, *34*(1), 17–30. http://dx.doi.org/10.5935/2236-3122.20130003.

Bi, J., Knyazikhin, Y., Choi, S., Park, T., Barichivich, J., Ciais, P., ... Myneni, R. B. (2015). Sunlight mediated seasonality in canopy structure and photosynthetic activity of Amazonian rainforests. *Environmental Research Letters*, *10*(6). http://dx.doi.org/10.1088/1748-9326/10/6/064014.

Brando, P. M., Goetz, S. J., Baccini, A., Nepstad, D. C., Beck, P. S. A., & Christman, M. C. (2010). Seasonal and interannual variability of climate and vegetation indices across the Amazon. *Proceedings of the National Academy of Sciences of the United States of America*, *107*(33), 14685–14690. http://dx.doi.org/10.1073/pnas.0908741107.

Cirino, G. G., Souza, R. A. F., Adams, D. K., & Artaxo, P. (2014). The effect of atmospheric aerosol particles and clouds on net ecosystem exchange in the Amazon. *Atmospheric Chemistry and Physics*, *14*, 6523–6543. http://dx.doi.org/10.5194/acp-14-6523-2014.

Coley, P. D., & Barone, J. A. (1996). Herbivory and plant defenses in tropical forests. *Annual Review of Ecology and Systematics*, *27*, 305–335.

Frias, G. A., Purdy, L. H., & Schmidt, R. A. (1991). Infection biology of *Crinipellis perniciosa* on vegetative flushes of cacao. *Plant Disease*, *75*(6), 552–556. http://dx.doi.org/10.1094/PD-75-0552.

Galvão, L. S., dos Santos, J. R., Roberts, D. A., Breunig, F. M., Toomey, M., & de Moura, Y. M. (2011). On intra-annual EVI variability in the dry season of tropical forest: A case study with MODIS and hyperspectral data. *Remote Sensing of Environment*, *115*(9), 2350–2359. http://dx.doi.org/10.1016/j.rse.2011.04.035.

Guan, K., Pan, M., Li, H., Wolf, A., Wu, J., Medvigy, D., ... Lyapustin, A. I. (2015). Photosynthetic seasonality of global tropical forests constrained by hydroclimate. *Nature Geoscience*, *8*(4), 284–289. http://dx.doi.org/10.1038/NGEO2382.

Marini, R. P., & Burden, J. A. (1987). Summer pruning of apple and peach trees. *Horticultural Reviews*, *9*, 351–375. http://dx.doi.org/10.1002/9781118060827.ch9.

Huete, A. R., Didan, K., Miura, T., Rodriguez, E. P., Gao, X., & Ferreira, L. G. (2002). Overview of the radiometric and biophysical performance of the MODIS vegetation indices. *Remote Sensing of Environment*, *83*, 195–213. http://dx.doi.org/10.1016/S0034-4257(02)00096-2.

Huete, A. R., Didan, K., Shimabukuro, Y. E., Ratana, P., Saleska, S. R., Hutyra, L. R., & Myneni, R. B. (2006). Amazon rainforests green-up with sunlight in dry season. *Geophysical Research Letters*, *33*(6), L06405. http://dx.doi.org/10.1029/2005GL025583.

Huete, A. R., Dye, D., Saleska, S. R., Restrepo-Coupe, N., Amaral, D., Didan, K., ... Araújo, A. (2011). Scaling photosynthesis in Amazonian ecosystems: From forest to savanna, from seasons to extreme events. *The FLUXNET workshop* (Retrieved from:) http://nature.berkeley.edu/biometlab/fluxnet2011/PDF_Posters/Huete_Saleska_Dye.pdf

Hufkens, K., Friedl, M., Sonnentag, O., Braswell, B. H., Milliman, T., & Richardson, A. D. (2012). Linking near-surface and satellite remote sensing measurements of deciduous broadleaf forest phenology. *Remote Sensing of Environment*, *117*, 307–321. http://dx.doi.org/10.1016/j.rse.2011.10.006.

Kositsup, B., Kasemsap, P., Thanisawanyangkura, S., Chairungsee, N., Satakhun, D., Teerawatanasuk, K., ... Thaler, P. (2010). Effect of leaf age and position on light-saturated CO_2 assimilation rate, photosynthetic capacity, and stomatal conductance in rubber trees. *Photosynthetica*, *48*(1), 67–78. http://dx.doi.org/10.1007/s11099-010-0010-y.

Lieberei, R. (2007). South American leaf blight of the rubber tree (*Hevea* spp.): New steps in plant domestication using physiological features and molecular markers. *Annals of Botany*, *100*, 1125–1142. http://dx.doi.org/10.1093/aob/mcm133.

Lyapustin, A. I., Wang, Y., Laszlo, I., Hilker, T. G., Hall, F., Sellers, P. J., & Korkin, S. V. (2012). Multiangleimplementation of atmospheric correction for MODIS (MAIAC): 3. Atmosphericcorrection. *Remote Sensing of Environment*, ***127***, 385–393. http://dx.doi.org/10.1016/j.rse.2012.09.002.

Maeda, E. E., Heiskanen, J., Aragão, L. E. O. C., & Rinne, J. (2014). Can MODIS EVI monitor ecosystem productivity in the Amazon rainforest? *Geophysical Research Letters*, *41*. http://dx.doi.org/10.1002/2014GL061535.

Morton, D. C., Nagol, J., Carabajal, C. C., Rosette, J., Palace, M., Cook, B. D., ... North, P. R. J. (2014). Amazon forests maintain consistent canopy structure and greenness during the dry season. *Nature*, *506*(7487), 221–224. http://dx.doi.org/10.1038/nature13006.

Murali, K. S., & Sukumar, R. (1993). Leaf flushing phenology and herbivory in a tropical dry deciduous forest, southern India. *Oecologia*, *94*, 114–119. http://dx.doi.org/10.1007/BF00317311.

Nelson, B. W., Tavares, J. V., Wu, J., Valeriano, D. M., Lopes, A. P., Marostica, S. F., ... Huete, A. (2014). Seasonality of Central Amazon Forest leaf flush using tower-mounted RGB camera. *American Geophysical Union fall meeting* (Retrieved from:) https://agu.confex.com/agu/fm14/meetingapp.cgi#Paper/7861

Oliveira, P. H. F., Artaxo, P., Pires, C., De Lucca, S., Procópio, A., Holben, B., ... Rocha, H. R. (2007). The effects of biomass burning aerosols and clouds on the CO_2 flux in Amazonia. *Tellus*, *59B*, 338–349. http://dx.doi.org/10.1111/j.1600-0889.2007.00270.x.

Reich, P. B., & Borchert, R. (1988). Changes with leaf age in stomatal function and water status of several tropical tree species. *Biotropica*, *20*(1), 60–69. http://dx.doi.org/10.2307/2388427.

Reich, P. B., Uhl, C., Walters, M. B., Prugh, L., & Ellsworth, D. S. (2004). Leaf demography and phenology in Amazonian rain forest: A census of 40,000 leaves of 23 tree species. *Ecological Monographs*, *74*(1), 3–23. http://dx.doi.org/10.1890/02-4047.

Restrepo-Coupe, N., Rocha, H. R. da, Hutyrae, L. R., Araujo, A. C. da, Borma, L. S., Christoffersen, B. O., … Saleska, S. R. (2013). What drives the seasonality of photosynthesis across the Amazon basin? A cross-site analysis of eddy flux tower measurements from the Brasil flux network. Agricultural and Forest Meteorology, 182, 128–144, http://dx.doi.org/10.1016/j.agrformet.2013.04.031.

Richardson, A. D., Braswell, B. H., Hollinger, D. Y., Jenkins, J. P., & Ollinger, S. V. (2009). Near-surface remote sensing of spatial and temporal variation in canopy phenology. *Ecological Applications*, *19*(6), 1417–1428. http://dx.doi.org/10.1890/08-2022.1.

Richardson, A. D., Jenkins, J. P., Braswell, B. H., Hollinger, D. Y., Ollinger, S. V., & Smith, M. L. (2007). Use of digital webcam images to track spring green-up in a deciduous broadleaf forest. *Oecologia*, *152*(2), 323–334. http://dx.doi.org/10.1007/s00442-006-0657-z.

Richardson, A. D., Klosterman, S., & Toomey, M. (2013). Near-surface sensor-derived phenology. In M. D. Schwartz (Ed.), *Phenology: An integrative environmental science* (pp. 413–430). Dordrecht: Springer Netherlands. http://dx.doi.org/10.1007/978-94-007-6925-0_22.

Saleska, S. R., Didan, K., Huete, A. R., & da Rocha, H. R. (2007). Amazon forests green-up during 2005 drought. *Science*, *318*(5850), 612. http://dx.doi.org/10.1126/science.1146663.

Saleska, S. R., Wu, J., Guan, K., Restrepo-Coupe, N., Nobre, A. D., Araujo, A., & Huete, A. R. (2016). Dry-season greening of Amazon forests. *Nature Brief Communication Arising*, *531*(7594), E4–E5. http://dx.doi.org/10.1038/nature16457.

Samanta, A., Ganguly, S., & Myneni, R. B. (2011). MODIS enhanced vegetation index data do not show greening of Amazon forests during the 2005 drought. *New Phytologist*, *189*(1), 11–15. http://dx.doi.org/10.1111/j.1469-8137.2010.03516.x.

Sonnentag, O., Hufkens, K., Teshera-Sterne, C., Young, A. M., Friedl, M., Braswell, B. H., ... Richardson, A. D. (2012). Digital repeat photography for phenological research in forest ecosystems. *Agricultural and Forest Meteorology*, *152*, 159–177. http://dx.doi.org/10.1016/j.agrformet.2011.09.009.

Tavares, J. V. (2013). Green-up na Estação Seca da Amazônia Central : Padrões sazonais da fenologia foliar de uma floresta de terra firme. *Instituto Nacional de Pesquisas da Amazonia* (Retrieved from:) http://bdtd.ibict.br/vufind/Record/INPA_475d708f7a5e3f4d12f318fffe93f574

Toomey, M., Roberts, D., & Nelson, B. (2009). The influence of epiphylls on remote sensing of humid forests. *Remote Sensing of Environment*, *113*(8), 1787–1798. http://dx.doi.org/10.1016/j.rse.2009.04.002.

Woebbecke, D. M., Meyer, G. E., Von Bargen, K., & Mortensen, D. A. (1995). Color indices for weed identification under various soil, residue, and lighting conditions. *Transactions of ASAE*, *38*(1), 259–269.

Wright, S. J., & Schaik, C. P. V. (1994). Light and the phenology of tropical trees. *The American Naturalist*, *143*(1), 192–199.

Wu, J., Albert, L. P., Lopes, A. P., Restrepo-Coupe, N., Hayek, M., Wiedemann, K. T., ... Saleska, S. R. (2016). Leaf development and demography explain photosynthetic seasonality in Amazon evergreen forests. *Science*, *351*(6276), 972–976. http://dx.doi.org/10.1126/science.aad5068.

Xiao, X., Hagen, S., Zhang, Q., Keller, M., & Moore, B. (2006). Detecting leaf phenology of seasonally moist tropical forests in South America with multi-temporal MODIS images. *Remote Sensing of Environment*, *103*, 465–473. http://dx.doi.org/10.1016/j.rse.2006.04.013.

Xiao, X., Zhang, Q., Saleska, S., Hutyra, L., Camargo, P. D., Wofsy, S., ... Moore, B. (2005). Satellite-based modeling of gross primary production in a seasonally moist tropical evergreen forest. *Remote Sensing of Environment*, *94*, 105–122. http://dx.doi.org/10.1016/j.rse.2004.08.015.

Yang, X., Tang, J., & Mustard, J. F. (2014). Beyond leaf color: Comparing camera-based phenological metrics with leaf biochemical, biophysical and spectral properties throughout the growing season of a temperate deciduous forest. *Journal of Geophysical Research – Biogeosciences*, *119*(3), 181–191. http://dx.doi.org/10.1002/2013JG002460.

Zuidema, P. A., Brienen, R. J. W., & Schongart, J. (2012). Tropical forest warming: looking backwards for more insights. *Trends in Ecology & Evolution*, *27*(4), 193–194. http://dx.doi.org/10.1016/j.tree.2011.12.007.